PHYSICAL REVIEW B **92**, 081201(R) (2015)

Topological nodal line semimetals with and without spin-orbital coupling

Chen Fang,[1,*] Yige Chen,[2,3] Hae-Young Kee,[2,3] and Liang Fu[1]

[1]*Department of Physics, Massachusetts Institute of Technology, Cambridge, Massachusetts 02139, USA*

[2]*Department of Physics, University of Toronto, Toronto, Ontario, Canada M5S1A7*

[3]*Canadian Institute for Advanced Research/Quantum Materials Program, Toronto, Ontario, Canada MSG 1Z8*

(Received 15 June 2015; published 10 August 2015)

We theoretically study three-dimensional topological semimetals (TSMs) with nodal lines protected by crystalline symmetries. Compared to TSMs with point nodes, e.g., Weyl semimetals and Dirac semimetals, where the conduction and the valence bands touch at discrete points, in these TSMs the two bands cross at closed lines in the Brillouin zone. We propose two different classes of symmetry protected nodal lines in the absence and in the presence of spin-orbital coupling (SOC), respectively. In the former, we discuss nodal lines that are protected by a combination of inversion symmetry and time-reversal symmetry, yet, unlike previously studied nodal lines in the same symmetry class, each nodal line has a Z_2 monopole charge and can only be created (annihilated) in pairs. In the second class, with SOC, we show that a nonsymmorphic symmetry (screw axis) protects a four-band crossing nodal line in systems having both inversion and time-reversal symmetries.

DOI: 10.1103/PhysRevB.92.081201 PACS number(s): 71.18.+y, 71.20.Be, 02.40.Re, 02.20.Bb

The study of topological semimetals has recently drawn much attention from both the theoretical and the experimental communities. Topological semimetals (TSMs) are systems where the conduction and the valence bands have robust crossing points in k space, compared with normal metals where the two bands have a direct gap at each $\mathbf{k}$. Compared with normal metals, the Fermi surface (FS) of an ideal TSM has a reduced dimension: In two dimensions, a normal metal has a one-dimensional (1D) FS while a TSM has a zero-dimensional (0D) FS; and in three dimensions, a normal metal has a two-dimensional (2D) FS while a TSM has a 1D or 0D FS. More importantly, the states near the FS are characterized by a nontrivial topological number. These unique features of FS in TSMs give rise to exotic properties, such as the existence of Fermi arcs on the surface [1] and the chiral anomaly in the bulk [2,3]. In three dimensions, Weyl semimetals [1] and Dirac semimetals [4] have been intensively studied both theoretically [2,5–13] and experimentally [14–25]. In Weyl semimetals, the two bands cross at an even number of discrete points in the Brillouin zone (BZ), around which the bands are nondegenerate and disperse linearly in all three directions. In Dirac semimetals, both the conduction and the valence bands are twofold degenerate and cross each other at an odd or even number of points. Both systems belong to the class of topological nodal point semimetals (TPSMs).

In three dimensions, there is another class of TSMs where the conduction and the valence bands cross each other at closed lines instead of discrete points, i.e., nodal lines [5,13,26–38]. These nodal line semimetals (TLSMs) are in the midway between TPSMs and normal metals: (i) At exact half filling, the FS is 0D, 1D, and 2D in TPSMs, TLSMs, and normal metals, and (ii) the density of state scales as $\rho_0 \propto (E - E_f)^2$, $\rho_0 \propto |E - E_f|$, and a constant in TPSMs, TLSMs, and normal metals, a fact from which one expects distinct electron correlation effects in the three classes. For example, the screening effect in these metallic states has been discussed [39]. Very recently, many theoretical proposals of materials for realizing TLSMs have emerged, including the realization in graphene networks [31], in Ca_3P_2 [32], in LaN [13], and in $Cu_3(Pd,Zn)N$ [33,34]. In all these works, and also in earlier theoretical model studies [5,27,28], the nodal line has the following properties: (i) Unlike a Weyl node, a single line node can shrink to a point and vanish by continuously tuning the Hamiltonian [33], and (ii) its stability requires the absence of spin-orbital coupling (SOC), and upon turning on strong SOC, each nodal line is either split or gapped due to the hybridization between opposite spin components [10,13]. It is natural to ask if there is another class of nodal lines with nontrivial monopole charges, and if there are nodal lines that are robust even in the presence of SOC, i.e., four-band crossing lines. These open questions motivate us to develop a more comprehensive theory on TLSMs.

Our results are presented in two parts on TLSMs without and with SOC, respectively. In the first part, we revisit systems with P and T in the absence of SOC, and find a different class of nodal lines that can only be created and annihilated in pairs, characterized by a unique Z_2 topological invariant. For a closed surface around the nodal line, we define a Z_2 invariant protected by $P * T$, classifying all nodal lines into two classes, with and without a Z_2 charge, respectively. Nodal lines with a Z_2 charge can only be created and annihilated in pairs, as the total charge of the BZ must be zero. Finite perturbation can make a nodal line with a Z_2 charge shrink to an accidental nodal point, but cannot gap it. In the second part, we discuss systems with P, T, and strong SOC. We show that if there is an additional twofold screw axis, a four-band crossing line, or a double nodal line (crossing between two doubly degenerate bands), can be protected on the boundary of the BZ. This is analytic proof of the symmetry protection of a four-band crossing line. We apply the resultant theory to explain the double nodal line found in earlier model studies [26,29] on $SrIrO_3$.

The symmetry we consider is the composition of P and T, or $P * T$, an antiunitary symmetry that preserves the momentum of a single particle. In a system without

*fangc@mit.edu

SOC, we have $T^2 = 1$, $P^2 = 1$, and $[P,T] = 0$, which imply $(P*T)^2 = +1$. The action of $P*T$ on the atomic orbitals can hence be represented by complex conjugation (K) up to a basis choice. Therefore, the single particle Hamiltonian $H(\mathbf{k})$ is a real matrix at every $\mathbf{k}$ in BZ. A real, gapped Hamiltonian has a Z_2 topological classification in both one and two dimensions, indicated by the first and the second homotopy groups of the projector onto the occupied bands [40],

$$\pi_1\left(\frac{O(M+N)}{O(M)\oplus O(N)}\right) = \pi_2\left(\frac{O(M+N)}{O(M)\oplus O(N)}\right) = Z_2, \quad (1)$$

where M and N are the numbers of the unoccupied and the occupied bands ($M,N > 1$). Since $H(\mathbf{k})$ is real, at each $\mathbf{k}$ there is a real representation for all eigenstates of $H(\mathbf{k})$. Therefore, for each projector onto the occupied bands $P(\mathbf{k})$, $1-2P(\mathbf{k})$ is an $O(M+N)$ matrix that is invariant under any rotation within the occupied (unoccupied) space, i.e., an element of the quotient group.

The Z_2 classification of $H(\mathbf{k})$ in 1D directly leads to protected nodal points in 2D and nodal lines in 3D, which have been studied in Refs. [5,31,33]. To see this, consider a closed path, i.e., a loop, in the 3D BZ, along which the Hamiltonian is gapped. The Z_2 invariant for the loop is simply the Berry's phase for all occupied bands, quantized to either 0 or π, corresponding to the trivial and the nontrivial classes, respectively. If a loop belongs to the nontrivial Z_2 class, it cannot shrink to a point and vanish without crossing a singularity. In 3D BZ, this implies a line of singularities threading through the loop [see Fig. 1(a)]. Given $H(\mathbf{k})$ continuous, each singularity is where the gap closes between the conduction and the valence bands, i.e., a nodal point, and a line of singularities is hence a nodal line. Given a nodal line in 3D, any loop that interlocks with the nodal line has a Berry's phase of π, while the other loops have zero Berry's phase. Thus we conclude that $P*T$ topologically protects a nodal line in 3D in the absence of SOC. Unlike the monopole charge of Weyl nodes, the 1D Z_2 invariant does not forbid a single nodal line from being annihilated or created locally in k space in 3D. Consider the following two-band model as an example:

$$H(\mathbf{k}) = (m - k^2)\sigma_x + k_z\sigma_z. \quad (2)$$

$H(\mathbf{k})$ has a nodal line on the $k_z = 0$ plane of radius $\sqrt{m}$ if $m > 0$. As we change m from positive to negative, the nodal line shrinks to a point at the origin and vanishes [see Fig. 1(c)]. The reverse process creates a single nodal line from the origin. This is a key difference between this nodal line and a point node in Weyl semimetal or some Dirac semimetal. In the latter cases, each point node has a monopole charge, and therefore can only be created or annihilated in pairs.

The nontrivial Z_2 classification for real, gapped Hamiltonians in 2D indicates a different classification for nodal lines in 3D. It implies that with $P*T$, $H(\mathbf{k})$ on the surface of a sphere can be topologically nontrivial. In 3D k space, if $H(\mathbf{k})$ on the surface of a sphere belongs to the nontrivial class, the sphere cannot shrink to a point and vanish without meeting a singularity. Since $P*T$ cannot stabilize a point node, the singularity is a nodal line inside the sphere.

The 2D Z_2 invariant for nodal lines in 3D k space, defined on a surface enclosing the line [see Fig. 1(b)], is a unique topological invariant. It indicates the absence or presence of the obstruction to finding a smooth and *real* gauge for the periodic part of the Bloch wave functions (wave functions for short hereafter) of the occupied bands. This invariant can be constructed based on this observation. Consider a sphere divided by an equator into two halves, say, the Northern and the Southern Hemispheres. The wave functions on each hemisphere, $|u_n^N(\theta,\phi)\rangle$ and $|u_n^S(\theta,\phi)\rangle$, can be real and smooth because each hemisphere is contractible. At each point on the equator, denoted by the azimuthal angle ϕ, where the two hemispheres meet, the projectors to the occupied space must be equal,

$$\sum_{n\in\text{occ}} \left|u_n^N\left(\frac{\pi}{2},\phi\right)\right\rangle\left\langle u_n^N\left(\frac{\pi}{2},\phi\right)\right| = \sum_{n\in\text{occ}} \left|u_n^S\left(\frac{\pi}{2},\phi\right)\right\rangle\left\langle u_n^S\left(\frac{\pi}{2},\phi\right)\right|,$$

because the Hamiltonian is smooth on the whole sphere. Therefore, the matrix

$$M_{mn}(\phi) = \left\langle u_m^N\left(\frac{\pi}{2},\phi\right)\middle| u_n^S\left(\frac{\pi}{2},\phi\right)\right\rangle \quad (3)$$

is an N_{occ}-by-N_{occ} orthogonal matrix. For the orthogonal group, there is

$$\pi_1[O(N_{\text{occ}})] = Z_2. \quad (4)$$

When $M(\phi)$ is Z_2 nontrivial, there is an obstruction to defining a smooth gauge on the whole sphere. In Sec. I of the Supplemental Material [41], we show how to obtain this invariant without using a smooth gauge on hemispheres.

This Z_2 invariant classifies nodal lines in 3D systems with $P*T$ into two classes: with and without a Z_2 charge. A nodal line with a Z_2 charge can be considered a Z_2 monopole, which can only be created or annihilated in pairs. This is easy to prove by contradiction: If a Z_2 monopole is created (annihilated) locally in k space, the wave functions sufficiently away from this point are changed by a small amount, so the Z_2 invariant on a surface far away from the point is unchanged, contradicting the assumption that a Z_2 monopole is created (annihilated) within.

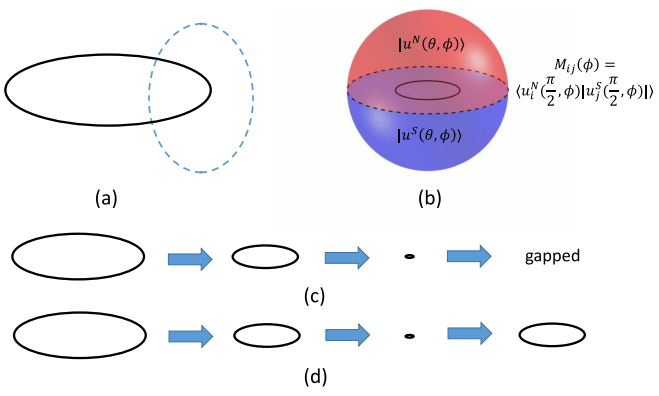

FIG. 1. (Color online) (a) A nontrivial Z_2 invariant (Berry's phase of π) of any loop in 3D BZ implies a nodal line (solid line) passing through the loop. (b) The 2D Z_2 invariant for a nodal line in 3D BZ defined on a sphere enclosing the line. (c) The evolution of a nodal line with zero monopole charge as the parameter changes in the model of Eq. (2). (d) The evolution of a nodal line with nonzero monopole charge as the parameter changes in the model of Eq. (5).

For concreteness, we construct a 3D Hamiltonian around such a Z_2 monopole,

$$H(\mathbf{k}) = q_x s_x + q_y \tau_y s_y + q_z s_z + m\tau_x s_x, \tag{5}$$

where τ_i and s_i are Pauli matrices acting on two isospin degrees of freedom and $\mathbf{q} \equiv \mathbf{k} - \mathbf{k}_0$ is the momentum relative to the origin of the $k \cdot p$ expansion. The spectrum is given by

$$E(\mathbf{k}) = \pm\sqrt{q_z^2 + \left(\sqrt{q_x^2 + q_y^2} \pm m\right)^2}. \tag{6}$$

The band crossing can be found by solving $E(\mathbf{q}) = 0$, yielding $k_z = 0$ and $\sqrt{q_x^2 + q_y^2} = |m|$, i.e., a nodal line on the xy plane of radius $\sqrt{|m|}$. As m changes from positive to negative, the radius decreases and shrinks to zero at $m = 0$, but increases again when m becomes negative [see Fig. 1(d)]. An explicit calculation of the Z_2 charge of this nodal line is given in Sec. II of the Supplemental Material [41].

We emphasize that the SU(2) rotation plays an important role in protecting a line node. When SU(2) is broken, or there is SOC, the composition of inversion and time reversal ensures double degeneracy at each $\mathbf{k}$ in BZ. Any crossing point between two doublet bands is hence a four-band crossing, yet it is easy to see that a four-band crossing is not protected in any 3D system without additional symmetries. Without SU(2), the symmetry $P * T$ satisfies $(P * T)^2 = -1$, because $T^2 = -1$ in a spin half system. A generic four-band model with $P * T$ in the presence of SOC is

$$H(\mathbf{k}) = f_1 s_x + f_2 \tau_y s_y + f_3 s_z + f_4 \tau_x s_y + f_5 \tau_z s_y, \tag{7}$$

where each f_i is a function of (k_x, k_y, k_z), $P * T = K(i\tau_y)$. A band crossing requires five equations to be satisfied, namely, $f_1 = f_2 = f_3 = f_4 = f_5 = 0$, which is impossible in a 3D BZ without fine tuning. It is natural to ask if additional symmetries can protect a four-band crossing nodal line in 3D systems with SOC, and further, if yes, what are they.

Recent work shows that in the presence of nonsymmorphic symmetries, four-band crossings can appear at high symmetry 0D nodal points on the BZ boundary [42]. A nonsymmorphic symmetry is a point group symmetry composed with a fractional lattice translation; the commutation relation involving a nonsymmorphic symmetry is generally k dependent due to the translation part [43–47]. At Γ, a nonsymmorphic symmetry can be treated as its point group component as long as the commutation relations are concerned; at a BZ boundary, the fractional translation makes the group structure of nonsymmorphic symmetries different from any point group, and leads to other types of band crossings and high degeneracies [48].

In this Rapid Communication we show that the presence of P, T, and a twofold screw axis protect double nodal lines (four-band crossing lines) on the BZ boundary in a 3D system with SOC. Unlike P that only acts in the real space, a twofold screw axis along z (S_z) acts in both the real space (x, y, z) and the spin space (s_x, s_y, s_z) simultaneously,

$$\begin{aligned} S_z : (x,y,z) &\to \left(-x + \frac{\mu a}{2}, -y + \frac{\lambda b}{2}, z - \frac{c}{2}\right), \\ (s_x, s_y, s_z) &\to (-s_x, -s_y, s_z), \end{aligned} \tag{8}$$

where $\mu, \lambda = 0, 1$ denote the shift of the axis $(\mu a/4, \lambda b/4, z)$ from the inversion center and a, b, and c are the lengths of three basis vectors. Combining the twofold axis and inversion generates another symmetry:

$$\begin{aligned} R_z : (x,y,z) &\to \left(x - \frac{\mu a}{2}, y - \frac{\lambda b}{2}, -z + \frac{c}{2}\right), \\ (s_x, s_y, s_z) &\to (-s_x, -s_y, s_z). \end{aligned} \tag{9}$$

R is a mirror plane (if $\mu = \lambda = 0$) or a glide plane (if μ or λ is nonzero) located at $z = c/4$. Consider the commutation relation between $P * T$ and R_z. In real space we have

$$\begin{aligned} (x,y,z,t) &\xrightarrow{R_z} \left(x - \frac{\mu a}{2}, y - \frac{\lambda b}{2}, -z + \frac{c}{2}, t\right) \\ &\xrightarrow{P*T} \left(-x + \frac{\mu a}{2}, -y + \frac{\lambda b}{2}, z - \frac{c}{2}, -t\right), \\ (x,y,z,t) &\xrightarrow{P*T} (-x, -y, -z, -t) \\ &\xrightarrow{R_z} \left(-x - \frac{\mu a}{2}, -y - \frac{\lambda b}{2}, z + \frac{c}{2}, -t\right), \end{aligned} \tag{10}$$

and in spin space

$$\begin{aligned} (s_x, s_y, s_z) &\xrightarrow{R_z} (-s_x, -s_y, s_z) \\ &\xrightarrow{P*T} (s_x, s_y, -s_z), \\ (s_x, s_y, s_z) &\xrightarrow{P*T} (-s_x, -s_y, -s_z) \\ &\xrightarrow{R_z} (s_x, s_y, -s_z), \end{aligned} \tag{11}$$

from which we find

$$\begin{aligned} R_z * (P * T) &= T_{(-\mu a, -\lambda b, c)} (P * T) * R_z \\ &= e^{-ik_z + i\mu k_x + i\lambda k_y} (P * T) * R_z. \end{aligned} \tag{12}$$

There are two planes (mirror invariant planes) defined by $k_z = 0$ and $k_z = \pi$ in the BZ that are invariant under R_z, on which the commutation relations given by Eq. (12) differ by a minus sign.

On each mirror invariant plane, the bands can be labeled by their respective R_z eigenvalues. In a system with SOC, we have

$$\begin{aligned} R_z^2 : (x,y,z) &\to (x - \mu a, y - \lambda b, z), \\ (s_x, s_y, s_z) &\to (s_x, s_y, s_z), \end{aligned} \tag{13}$$

or

$$R_z^2 = -T_{-\mu a, -\lambda b, 0} = -e^{i\mu k_x + i\lambda k_y}. \tag{14}$$

The minus sign is because R_z is equivalent to a π rotation along z in the spin space so R_z^2 includes a 2π rotation, giving a -1 for a spin-1/2 system. Therefore, each band at $k_z = 0$ and $k_z = \pi$ either has an R_z eigenvalue $g_+ = +ie^{(i\mu k_x + i\lambda k_y)/2}$ or $g_- = -g_+$. In the presence of SOC and $P * T$, bands are doubly degenerate, and the degenerate bands are related to each other by $P * T$. Suppose at (k_x, k_y, k_0), where $k_0 = 0, \pi$, a Bloch function $|\psi(\mathbf{k})\rangle$ is an eigenstate of R_z with eigenvalue g_+, then we consider its degenerate partner $P * T|\psi(\mathbf{k})\rangle$

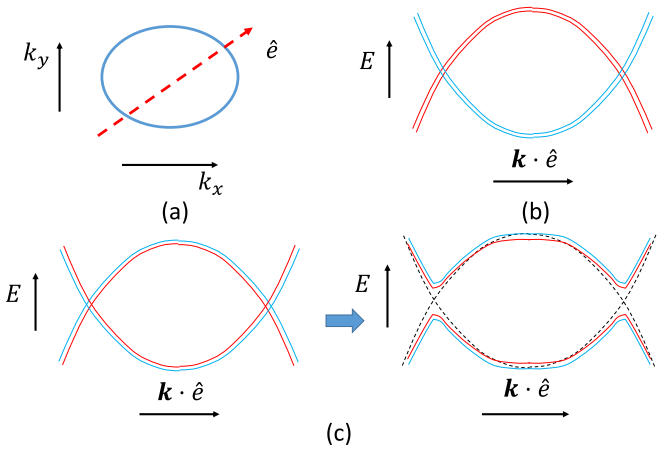

FIG. 2. (Color online) (a) A band crossing line on some mirror invariant plane at $k_z = 0$ or $k_z = \pi$, with an arbitrary cut along which the band structure is plotted. (b) The band structure along the cut in (a) on $k_z = \pi$, with the corresponding eigenvalues of R_z shown, where the degenerate states of a doublet band have the same eigenvalue. (c) The same band structure on $k_z = 0$, where the degenerate states of a doublet band have opposite R_z eigenvalues, which can anticross with another doublet band due to the spin mixing enabled by SOC.

under R_z,

$$\begin{aligned} R_z(P*T)|\psi(\mathbf{k})\rangle &= e^{-ik_0+i\mu k_x+i\lambda k_y}(P*T)R_z|\psi(\mathbf{k})\rangle \\ &= e^{-ik_0+i\mu k_x+i\lambda k_y}P*Tg_+|\psi(\mathbf{k})\rangle \\ &= e^{-ik_0}g_-P*T|\psi(\mathbf{k})\rangle. \end{aligned}$$

At $k_0 = 0$, the degenerate bands have opposite R_z eigenvalues, and two sets of such doublet bands generally anticross: The bands with the same R_z eigenvalue hybridize and avoid crossing [see Fig. 2(c)]. At $k_0 = \pi$, however, the degenerate bands have the same R_z eigenvalue. In this case, two doublet bands with opposite R_z eigenvalues may cross each other along a nodal line, making a symmetry protected four-band crossing line, or a double nodal line [see Fig. 2(b)]. In Sec. III of the Supplemental Material [41], we revisit the 3D $k\cdot p$ model in Eq. (7) in the presence of R_z in addition to $P*T$ and show the presence of a double nodal line, and in Sec. IV, we write down a formal invariant for the double nodal lines.

We apply the theory for double nodal lines to the case of the iridate $SrIrO_3$. An eight-band tight-binding model consistent with all symmetries in the space group has been shown to exhibit the double line [26,29,35] around point U in BZ, but a general symmetry analysis for an arbitrary number of bands is missing to pin down which symmetries of the little group at U are protecting the double nodal line, whereas the other symmetries may be broken without opening a gap or splitting the double line into two single nodal lines and/or point nodes.

The little group at U is generated by P plus two screw axes:

$$\begin{aligned} P &: (x,y,z) \to (-x,-y,-z), \\ S_y &: (x,y,z) \to (-x+a/2, y+b/2, -z+c/2), \\ S_z &: (x,y,z) \to (-x,-y,z+c/2). \end{aligned} \quad (15)$$

Following our theory, we see that P, T, and S_y (S_z) can protect double nodal lines on the $k_y = \pi$ ($k_z = \pi$) plane. Therefore, the double nodal line predicted in Ref. [26] on the $k_y = \pi$ plane is protected by P, T, and S_y. The other symmetries, including S_z, $S_x = S_y * S_z$, $M_z = S_z * P$, and $G_b = P * S_x$, may all be broken without gapping or splitting the double line. These statements may be tested in future experiments, as the crystalline symmetries can be modified by applying epitaxial strain on thin-film samples [49].

We briefly comment on the possibility of surface states in the TLSMs proposed. The protection of the nodal lines in this work requires the presence of P, as opposed to the Weyl semimetals where no symmetry (other than translation) is required. Since an open surface always breaks the inversion, no protected surface states, strictly speaking, are associated with these TLSMs; however, as shown in Refs. [29,31], when the conduction and the valence bands are nearly symmetric, there is a nearly flat surface band bounded by the projection of the nodal line [50].

We propose two different classes of three-dimensional topological semimetals with nodal lines in systems with and without spin-orbital coupling. Without spin-orbital coupling, or equivalently, with SU(2) spin rotation symmetry, inversion and time reversal can protect a nodal line that carries a Z_2 monopole charge, independent of the previously known π Berry's phase. Nodal lines with a nonzero monopole charge can only be created or annihilated in pairs, while the nodal lines in previous studies can be singly created and annihilated. In the presence of SOC, we prove that inversion plus time reversal is insufficient to protect any band crossing in 3D, and an additional nonsymmorphic symmetry (twofold screw axis) can protect a double nodal line, where two sets of doubly degenerate bands cross each other. We apply the theory to $SrIrO_3$, and identify symmetries required to protect the four-band crossing found in earlier model studies, and also symmetries that can be broken without gapping or splitting the double nodal line.

C.F. thanks A. Alexandradinata and B. A. Bernevig for useful discussion on the Wilson line technique used in the Supplemental Material, and C.-K. Chiu and S. Ryu for early discussions on the homotopy groups. C.F. and L.F. were supported by the S3TEC Solid State Solar Thermal Energy Conversion Center, an Energy Frontier Research Center funded by the U.S. Department of Energy (DOE), Office of Science, Basic Energy Sciences (BES), under Award No. DE-SC0001299/DE-FG02-09ER46577. Y.C. and H.Y.K. were supported by the NSERC of Canada and the Centre for Quantum Materials at the University of Toronto.

[1] X. Wan, A. M. Turner, A. Vishwanath, and S. Y. Savrasov, Phys. Rev. B **83**, 205101 (2011).

[2] P. Hosur, S. A. Parameswaran, and A. Vishwanath, Phys. Rev. Lett. **108**, 046602 (2012).

[3] D. T. Son and B. Z. Spivak, Phys. Rev. B **88**, 104412 (2013).
[4] S. M. Young, S. Zaheer, J. C. Y. Teo, C. L. Kane, E. J. Mele, and A. M. Rappe, Phys. Rev. Lett. **108**, 140405 (2012).
[5] A. A. Burkov, M. D. Hook, and L. Balents, Phys. Rev. B **84**, 235126 (2011).
[6] A. A. Burkov and L. Balents, Phys. Rev. Lett. **107**, 127205 (2011).
[7] C. Fang, M. J. Gilbert, X. Dai, and B. A. Bernevig, Phys. Rev. Lett. **108**, 266802 (2012).
[8] C.-X. Liu, P. Ye, and X.-L. Qi, Phys. Rev. B **87**, 235306 (2013).
[9] L. Lu, L. Fu, J. D. Joannopoulos, and M. Soljacic, Nat. Photon. **8**, 821 (2013).
[10] H. Weng, C. Fang, Z. Fang, B. A. Bernevig, and X. Dai, Phys. Rev. X **5**, 011029 (2015).
[11] S.-M. Huang, S.-Y. Xu, I. Belopolski, C.-C. Lee, G. Chang, B. Wang, N. Alidoust, G. Bian, M. Neupane, A. Bansil *et al.*, Nat. Commun. **6**, 7373 (2015).
[12] Z. Wang, Y. Sun, X.-Q. Chen, C. Franchini, G. Xu, H. Weng, X. Dai, and Z. Fang, Phys. Rev. B **85**, 195320 (2012).
[13] M. Zeng, C. Fang, G. Chang, Y.-A. Chen, T. Hsieh, A. Bansil, H. Lin, and L. Fu, arXiv:1504.03492.
[14] L. Lu, Z. Wang, D. Ye, L. Ran, L. Fu, J. D. Joannopoulos, and M. Soljačić, Science **349**, 622 (2015).
[15] S.-Y. Xu, I. Belopolski, N. Alidoust, M. Neupane, G. Bian, C. Zhang, R. Sankar, G. Chang, Z. Yuan, C.-C. Lee *et al.*, Science **349**, 613 (2015).
[16] B. Q. Lv, H. M. Weng, B. B. Fu, X. P. Wang, H. Miao, J. Ma, P. Richard, X. C. Huang, L. X. Zhao, G. F. Chen *et al.*, Phys. Rev. X **5**, 031013 (2015).
[17] C. Zhang, Z. Yuan, S.-Y. Xu, Z. Lin, B. Tong, M. Z. Hasan, J. Wang, C. Zhang, and S. Jia, arXiv:1502.00251.
[18] X. Huang, L. Zhao, Y. Long, P. Wang, D. Chen, Z. Yang, H. Liang, M. Xue, H. Weng, Z. Fang *et al.*, arXiv:1503.01304.
[19] Z. K. Liu, J. Jiang, B. Zhou, Z. J. Wang, Y. Zhang, H. M. Weng, D. Prabhakaran, S.-K. Mo, H. Peng, P. Dudin *et al.*, Nat. Mater. **13**, 677 (2014).
[20] Z. K. Liu, B. Zhou, Y. Zhang, Z. J. Wang, H. M. Weng, D. Prabhakaran, S.-K. Mo, Z. X. Shen, Z. Fang, X. Dai *et al.*, Science **343**, 864 (2014).
[21] M. Neupane, S.-Y. Xu, R. Sankar, N. Alidoust, G. Bian, C. Liu, I. Belopolski, T.-R. Chang, H.-T. Jeng, H. Lin *et al.*, Nat. Commun. **5**, 3786 (2014).
[22] L. P. He, X. C. Hong, J. K. Dong, J. Pan, Z. Zhang, J. Zhang, and S. Y. Li, Phys. Rev. Lett. **113**, 246402 (2014).
[23] S. Jeon, B. B. Zhou, A. Gyenis, B. E. Feldman, I. Kimchi, A. C. Potter, Q. D. Gibson, R. J. Cava, A. Vishwanath, and A. Yazdani, Nat. Mater. **13**, 851 (2014).
[24] S.-Y. Xu, C. Liu, S. K. Kushwaha, R. Sankar, J. W. Krizan, I. Belopolski, M. Neupane, G. Bian, N. Alidoust, T.-R. Chang *et al.*, Science **347**, 294 (2015).
[25] J. Xiong, S. Kushwaha, J. Krizan, T. Liang, R. J. Cava, and N. P. Ong, arXiv:1502.06266.
[26] J.-M. Carter, V. V. Shankar, M. A. Zeb, and H.-Y. Kee, Phys. Rev. B **85**, 115105 (2012).
[27] C.-K. Chiu and A. P. Schnyder, Phys. Rev. B **90**, 205136 (2014).
[28] M. Phillips and V. Aji, Phys. Rev. B **90**, 115111 (2014).
[29] Y. Chen, Y.-M. Lu, and H.-Y. Kee, Nat. Commun. **6**, 6593 (2015).
[30] K. Mullen, B. Uchoa, and D. T. Glatzhofer, Phys. Rev. Lett. **115**, 026403 (2015).
[31] H. Weng, Y. Liang, Q. Xu, Y. Rui, Z. Fang, X. Dai, and Y. Kawazoe, Phys. Rev. B **92**, 045108 (2015).
[32] L. S. Xie, L. M. Schoop, E. M. Seibel, Q. D. Gibson, W. Xie, and R. J. Cava, APL Mater. **3**, 083602 (2015).
[33] Y. Kim, B. J. Wieder, C. L. Kane, and A. M. Rappe, Phys. Rev. Lett. **115**, 036806 (2015).
[34] R. Yu, H. Weng, Z. Fang, X. Dai, and X. Hu, Phys. Rev. Lett. **115**, 036807 (2015).
[35] J.-W. Rhim and Y. B. Kim, Phys. Rev. B **92**, 045126 (2015).
[36] C.-K. Chiu, J. C. Y. Teo, A. P. Schnyder, and S. Ryu, arXiv:1505.03535.
[37] G. Bian, T.-R. Chang, R. Sankar, S.-Y. Xu, H. Zheng, T. Neupert, C.-K. Chiu, S.-M. Huang, G. Chang, I. Belopolski *et al.*, arXiv:1505.03069.
[38] Y. Chen, Y. Xie, S. A. Yang, H. Pan, F. Zhang, M. L. Cohen, and S. Zhang, arXiv:1505.02284.
[39] Y. Huh, E.-G. Moon, and Y. B. Kim, arXiv:1506.05105.
[40] A. Hatcher, *Algebraic Topology* (Cambridge University Press, Cambridge, UK, 2002).
[41] See Supplemental Material at http://link.aps.org/supplemental/10.1103/PhysRevB.92.081201 for (i) an explicit expression for the Z_2 invariant without using a smooth gauge on the hemispheres, (ii) explicit calculation of the Z_2 invariant for the model given in Eq. (5), (iii) proof of the existence of a protected double nodal line in the model given in Eq. (7) in the presence of P, T, and a twofold screw axis, and (iv) a formal definition of the topological invariant for a double nodal line.
[42] S. M. Young and C. L. Kane, arXiv:1504.07977.
[43] S. A. Parameswaran, A. M. Turner, D. P. Arovas, and A. Vishwanath, Nat. Phys. **9**, 299 (2013).
[44] C.-X. Liu, R.-X. Zhang, and B. K. VanLeeuwen, Phys. Rev. B **90**, 085304 (2014).
[45] C. Fang and L. Fu, Phys. Rev. B **91**, 161105 (2015).
[46] K. Shiozaki, M. Sato, and K. Gomi, Phys. Rev. B **91**, 155120 (2015).
[47] H. Watanabe, H. C. Po, A. Vishwanath, and M. P. Zaletel, arXiv:1505.04193.
[48] C. Bradley and A. Cracknell, *The Mathematical Theory of Symmetry in Solids: Representation Theory for Point Groups and Space Groups* (Oxford University Press, Oxford, UK, 2010).
[49] J. Liu, D. Kriegner, L. Horak, D. Puggioni, C. R. Serrao, D. Yi, C. Frontera, V. Holy, A. Vishwanath, J. M. Rondinelli *et al.*, arXiv:1506.03559.
[50] The surface flat band proposed in $SrIrO_3$ is protected by the mirror symmetry M_z and an approximate chiral symmetry specific to this system [29]. The chiral symmetry makes the conduction and the valence bands symmetric in energy.